

Effect of vortex handedness on spin momentum torque dynamics in dual-vortex ferromagnetic nanopillar structures

J. G. Deak^{a)}

NVE Corporation, 11409 Valley View Road, Eden Prairie, Minnesota 55344, USA

(Presented on 9 November 2007; received 14 September 2007; accepted 20 November 2007; published online 2 April 2008)

An investigation of the dynamics of vortices driven by spin-momentum transfer in magnetic tunnel junction nanopillars containing a vortex in the hard ferromagnetic pinned layer (PL) and a vortex in the soft ferromagnetic free layer (FL) is presented. This dual vortex configuration is interesting because the handedness of the vortex in the PL can be set so that the SMT is either assisted or opposed by the torque due to the Amperean magnetic field produced by the current passing through the nanopillar. It is shown that the handedness of the vortex in the PL controls the dynamics of the nanopillar device. Micromagnetic simulations of the three-dimensional nanopillar structures were performed as a function of PL vortex handedness, spin polarization (η), and nanopillar dimensions. Generally, for positive η , it is found that when the PL vortex is set counter-clockwise (CCW), the FL vortex shows a well-defined switching behavior, where the handedness of the final vortex state in the FL is dependent on the current direction through the nanopillar, and the switching current is decreased as η is increased. In devices where the PL is magnetized clockwise (CW), the FL magnetization dynamics show a more complicated dependence on η . The CW magnetized PL nanopillars show high-current Amperean field-induced vortex switching at low η , chaotic oscillation at intermediate η , and well-defined low-current switching at high η . For negative η , the CCW and CW PL results invert. © 2008 American Institute of Physics.

[DOI: [10.1063/1.2838016](https://doi.org/10.1063/1.2838016)]

Spin momentum transfer (SMT) describes the transfer of spin angular momentum between a spin-polarized current and a ferromagnet.¹ The transfer of angular momentum from the spin current to the ferromagnet exerts a torque on the magnetization of the ferromagnet. The SMT torque can be used to reverse the direction of the magnetization or to induce microwave oscillation of the magnetization of a ferromagnet. SMT can, thus, be applied to the free layer of a magnetic tunnel junction (MTJ) or vertical giant magnetoresistive structure in order to produce oscillators or magnetic memory devices.²⁻⁴

The SMT effect has been studied in uniformly magnetized nanopillar devices in the presence of uniform applied fields. The devices are usually patterned with dimensions of less than about 200 nm.³⁻⁵ Unfortunately, in this size range it may be energetically favorable for the ferromagnetic layers to magnetize into vortices as thickness is increased above about 5 nm.⁶ To make matters worse, the current flowing through the nanopillars produces a magnetic field that reinforces the vortex state. The work is thus intended to study the effect of vortices on SMT dynamics. Structures with a vortex set in the hard layer and with sufficiently thick freelaye to form a vortex are thus simulated. It is found that the direction of the magnetization in the pinned layer, either clockwise (CW) or counter-clockwise (CCW) determines the type of dynamic behavior the dual vortex nanopillar will experience. This dual-vortex scheme appears to provide a means to

fabricate either memory or oscillator SMT nanopillar devices without the need for external bias fields.

Figure 1 shows the geometry used for a SMT nanopillar. The current I becomes spin polarized through two effects, one is by transmission through a ferromagnetic layer and the other is by reflection off a ferromagnetic layer that is magnetized in the direction opposite to the electron's spin. The equation used to describe the dynamical response of a magnetic moment to a magnetic field and spin-polarized current is the Landau-Lifshitz-Gilbert (LLG) equation, with the addition of a term H_s , which represents the effective field from spin-polarized current,

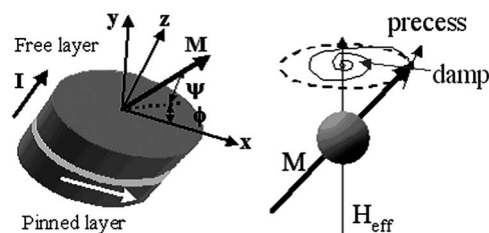


FIG. 1. (Left) A three layer stack composed of a magnetically pinned or fixed layer ferromagnet, where the magnetization is fixed along one direction, a nonmagnetic-spacer layer, and a ferromagnetic free layer, where the magnetization is free to rotate. The angle ψ describes the rotation of the magnetization out of the plane of the ferromagnetic film, and the angle ϕ describes the rotation in the plane of the film. The current I flows perpendicularly through the spacer layer, traversing both the free and pinned layers. (Right) Precession of a magnetic moment about an applied field as described by Eq. (1).

^{a)}Electronic mail: jdeak@nve.com.

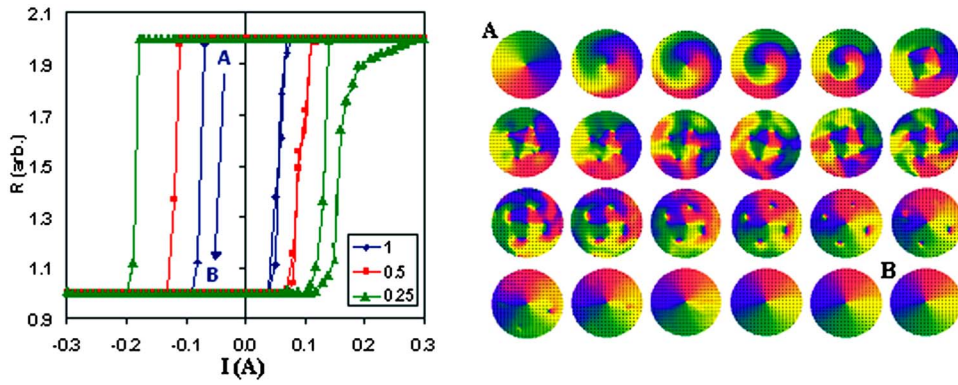


FIG. 2. (Color online) Simulation of dual-vortex nanopillars having a CCW vortex set in the pinned layer as a function of η , and evolution of the magnetization in the free layer during SMT reversal when the pinned layer is set CCW and $\eta = -1$. The magnetization stabilizes at high current. A snapshot is acquired at each 0.025 ns. Note that increasing spin polarization decreases the switching current.

$$\frac{(1 + \alpha^2) d\hat{m}}{\mu_0 \gamma dt} = -\hat{m} \times \mathbf{H} - \alpha \hat{m} \times \hat{m} \times (\mathbf{H} + \mathbf{H}_s). \quad (1)$$

$$\mathbf{H}_s = \left(\frac{\hbar}{2e} \right) \left(\frac{\eta I}{\alpha M_s V} \right) \hat{x}, \quad (4)$$

The general behavior of this equation is that after application of a field H the magnetization, $\mathbf{M} = M_s \hat{m}$, will precess around \mathbf{H} and the precessional cone angle will gradually decrease as \mathbf{M} aligns with \mathbf{H} . In Eq. (1), the term on the left represents the rate of change of \mathbf{M} , the first term on the right describes the natural tendency for a magnetic moment to precess around a magnetic field, and the second term on the right describes the damping of the precession as energy is dissipated. The constant that describes the rate of damping is α .

In this monodomain zero-temperature example, the effective field \mathbf{H} is given in terms of an externally applied field and the demagnetizing field of the free layer,

$$\mathbf{H} = [H_x - N_x M_s \cos(\Psi) \cos(\varphi)] \hat{x} - N_y M_s \cos(\Psi) \sin(\varphi) \hat{y} - N_z M_s \sin(\Psi) \hat{z}. \quad (2)$$

Here, the constants N_x , N_y , and N_z describe the demagnetizing field and can also be used to describe magnetic anisotropy. The effective field is dependent on the orientation of \mathbf{M} , and the unit vector representing the direction of the magnetization of the free layer is given in terms of the angles ψ and φ as follows:

$$\hat{m} = \cos(\psi) \cos(\varphi) \hat{x} + \cos(\psi) \sin(\varphi) \hat{y} + \sin(\psi) \hat{z}. \quad (3)$$

SMT is incorporated into the LLG equation as an effective field from spin-polarized current, which is given as

where e is the electron charge, \hbar is Planck's constant, V the volume of the free layer, and η is the degree of spin polarization of the applied current I .

The magnetization reversal mechanism due to SMT is quite different from that due to a magnetic field alone. In the case of a spin-polarized current, SMT causes a reduction in damping which allows spin waves to grow as long as current is supplied and the orientation of \mathbf{M} does not cross beyond the hard axis of the ferromagnetic film. To understand how SMT causes magnetization reversal, it is useful to solve an equation in the case where the precession angle is small. This permits the equation to be linearized into a second-order differential equation that is analogous to a damped harmonic oscillator,

$$\frac{(1 + \alpha^2)}{\mu_0 M_s \gamma} \phi'' + \alpha \left\{ (N_z + N_y - 2N_x) + \frac{2(H_x + H_s)}{M_s} \right\} \phi' + \frac{\mu_0 M_s \gamma}{(1 + \alpha^2)} \left\{ (N_z - N_x) \frac{H_x}{M_s} \right\} \left\{ (N_y - N_x) + \frac{H_x}{M_s} \right\} \phi = 0. \quad (5)$$

The magnitude and sign of the second term determine the oscillatory behavior of the magnetization. The second term becomes negative if

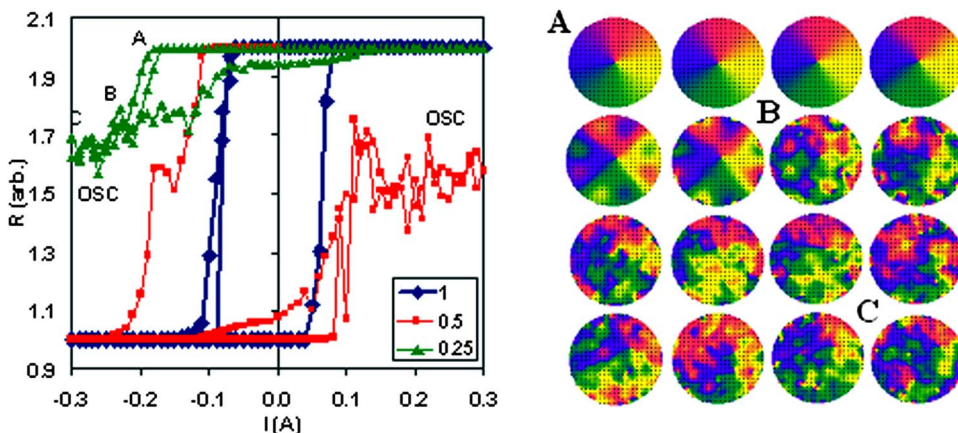


FIG. 3. (Color online) Simulation of dual-vortex nanopillars having a CW vortex set in the pinned layer as a function of η , and evolution of the magnetization in the free layer during SMT reversal when the pinned layer is set CW and $\eta = -0.25$. The magnetization dynamics become chaotic at high current and the device oscillates at high frequency. A snapshot is acquired each at 0.25 ns. Note that increasing spin polarization decreases the switching current, but improves the switching characteristics.

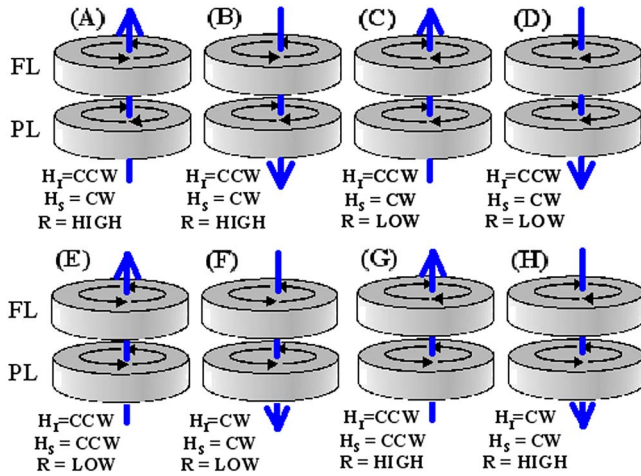


FIG. 4. (Color online) The effective field and resistance that result in dual-vortex nanopillar devices as a function of the orientation of the FL and PL magnetization and current applied through the device. Polarization is assumed to be negative to make visualization easier—transmitted spin current and electrical current are, thus, in the same direction. Note that the CW device produces S_I and S_H effective fields that tend to oppose each other. [(A)–(D)] PL=CW. [(E)–(H)] PL=CCW.

$$|I_c| = \left(\frac{\alpha \mu_0 M_s^2 V}{\eta} \right) \left(\frac{2e}{\hbar} \right) \left\{ \frac{(N_y + N_z)}{2} - N_x + \frac{H_x}{M_s} \right\}, \quad (6)$$

and the precession angle would, thus, grow with increasing time, eventually increasing past the equator causing \mathbf{M} to reverse direction. Once the direction of \mathbf{M} is reversed, the damping becomes positive and \mathbf{M} stabilizes in the new orientation. Reversing the polarity of the current causes \mathbf{M} to switch into the opposite direction. Note that the zero-temperature monodomain solution is dependent on the polarity of the applied field H_x , which can increase or decrease I_c .

For the dual-vortex structure proposed herein, micromagnetic simulation is needed to account for nonuniform magnetization of the ferromagnetic layers and also for the nonuniform field produced by the current flowing through the nanopillar. This micromagnetic model has been described in Ref. 6. The simulated stack is a FM (ferromagnet)/nonmagnetic-spacer/FM/AF (anti-FM) nanopillar of circular cross section ranging from 100 to 400 nm on a 5 nm cubic mesh. The FM/AF pinned layer is frozen into a vortex, and the pinning field of 500 Oe is oriented at each site in the mesh in order to reinforce the vortex state. The FM layers have $M_s = 8 \times 10^5$ A/m, $A = 1 \times 10^{-11}$ J/m, and $\alpha = 0.02$. The spin polarization of the FM layers, η , is varied from 1 to -1 .

Typical simulation results for a dual-vortex nanopillar are shown in Figs. 2 and 3 as a function of current through the nanopillar and for pinned layers set in CW and CCW orientations. Generally, in terms of the switching behavior, we find that in the CW case, switching is worse and oscillation is more likely. Increasing η improves the switching behavior of the device as it stabilizes at fields lower than the onset of oscillation. In CCW devices, because of the polarity of the current-induced magnetic field compared to the spin polarization, oscillation does not occur for any value of η at

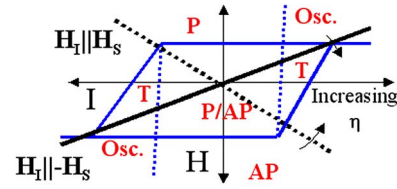


FIG. 5. (Color online) A phase diagram similar to that in Ref. 4. I refers to the current through the nanopillar, and H is the applied field. Here, “P” and “AP” refer to parallel and antiparallel orientation of the FL and PL, “osc.” refers to a regime where the nanopillar oscillates, and “T” refers to the regime where there is random telegraph noise. The lines labeled $H_I \parallel H_S$ and $H_I \parallel -H_S$ describe the contour probed when using a dual-vortex nanopillar device using a CCW or CW PL. The $H_I \parallel -H_S$ or simulated CW PL is more prone to oscillation. Increasing η causes the operating contours to rotate towards the “T” axis.

the currents studied. The magnetization patterns that occur during reversal in the CW and CCW pinned layer orientations are quite interesting, and they are shown along with the $R(I)$ loops in Figs. 2 and 3. Switching time was found to range from 0.3 to 10 ns, dependent on current and temperature.

With negative η , it appears that for the CCW PL vortex sense, the H field produced by the spin-polarized current reinforces the SMT effect, and for the CCW sense, it opposes SMT reversal. To make this clear, the different configurations and associated effective fields are illustrated in Fig. 4. The dependence of the dynamics on the CCW and CW PL reverses as the polarity of η is reversed in the simulation.

A phase diagram that explains the dependence of the dual-vortex nanopillar’s dynamics on the sense of the magnetization of the PL vortex is given in Fig. 5. This phase diagram is in the spirit of the experimental phase diagram found in Ref. 4. The $H_I \parallel -H_S$ and $H_I \parallel H_S$ contours that pass through the I and II and III and IV quadrants represent the operation of the dual-vortex nanopillar devices as the current is swept. Because the sense of the PL vortex changes the polarity of the H_I with respect to the H_S , and the H_I and H_S fields are both proportional to I through the nanopillar, the operating contours must traverse different diagonal quadrants. The $H_I \parallel H_S$ devices should perform better as memory elements as they do not pass through the oscillation regions at moderate to large η values, and the $H_I \parallel -H_S$ devices should perform better as oscillators, since the operating contours pass through the oscillation regions at moderate to high I for all η values. These results suggest PL vortex handedness needs to be controlled for optimal device operation.

¹J. Slonczewski, *J. Magn. Magn. Mater.* **159**, L1 (1996).

²D. Bussman, G. Prinz, S. Cheng, J. Zhu, Y. Zheng, J. Daughton, R. Beech, D. Wang, and R. Womack, “Current Perpendicular-To-Plane GMR for Magnetoresistive RAM”, Paper GA-03, presented at the 1999 Intermag Conference in Kyongju, Korea, May 1999; J. Zhu, Y. Zheng, and G. Prinz, *J. Appl. Phys.* **87**, 6668 (2000).

³V. S. Pribiag, I. N. Krivorotov, G. D. Fuchs, P. M. Braganca, O. Ozatay, J. C. Sankey, D. C. Ralph, and R. A. Burhman, *Nat. Phys.* **3**, 498 (2007).

⁴I. N. Krivorotov, N. C. Emley, A. G. F. Garcia, J. C. Sankey, D. C. Ralph, S. I. Kiselev, and R. A. Burhman, *Phys. Rev. Lett.* **93**, 166603 (2004).

⁵J. Deak, *J. Appl. Phys.* **97**, 10E316 (2005).

⁶J. G. Deak, *IEEE Trans. Magn.* **39**, 2510 (2003).